Curcumin-Loaded Chitosan Nanoparticle Preparation and Its Protective Effect on Celecoxib-induced...

DOI 10.1055/a-1960-3092
Drug Res

Publisher and Copyright:
© 2022 . Thieme. All rights reserved.
Georg Thieme Verlag KG, Rüdigerstraße 14,
70469 Stuttgart, Germany
ISSN 2194-9379

Thieme

Curcumin-Loaded Chitosan Nanoparticle Preparation and Its Protective Effect on Celecoxib-induced Toxicity in Rat isolated Cardiomyocytes and Mitochondria

Authors
Hossein Ali Ebrahimi[1], Samira Esmaeli[1], Saleh Khezri[2, 3], Ahmad Salimi[2, 3]

Affiliations
1 Department of Pharmaceutics, School of Pharmacy, Ardabil University of Medical Sciences, Ardabil, Iran
2 Traditional Medicine and Hydrotherapy Research Center, Ardabil University of Medical Sciences
3 Department of Pharmacology and Toxicology, School of Pharmacy, Ardabil University of Medical Sciences, Ardabil, Iran

Key word
nanotechnology, solid lipid nanoparticles, chitosan, celecoxib, curcumin, cardiotoxicity

received 14.06.2022
accepted 12.10.2022
published online 2022

Bibliography
Drug Res
DOI 10.1055/a-1960-3092
ISSN 2194-9379

Georg Thieme Verlag, Rüdigerstraße 14,
70469 Stuttgart, Germany

Correspondence
Ahmad Salimi
Associate Professor of Toxicology and Pharmacology School of Pharmacy
Ardabil University of Medical Sciences,
Ardabil: 56189-53141
Iran
Tel.: + 98(45)3352-3833, Fax: + 98(45)3352-2197
salimikd@yahoo.com,
a.salimi@pharmacy.arums.ac.ir

ABSTRACT

Curcumin has a wide range of pharmacological activities, including antioxidant, anti-inflammatory and tissue protective. In here we hypothesized that curcumin-loaded chitosan-coated solid lipid nanoparticles (CuCsSLN) are able to increase its overall bioavailability and hence its antioxidant and mitochondria;/lysosomal protective properties of curcumin. CuCsSLN were prepared using solvent diffusion technique for formation of solid lipid nanoparticles (SLNs) and electrostatic coating of positive-charged chitosan to negative surface of SLNs. CuCsSLN showed the encapsulation efficiency of 91.4 ± 2.7 %, the mean particle size of 208 ± 9 nm, the polydispersity index of 0.34 ± 0.07, and the zeta potential of + 53.5 ± 3.7 mV. The scanning electron microscope (SEM) images of nanoparticles verified their nanometric size and also spherical shape. Curcumin was released from CuCsSLN in a sustain release pattern up to 24 hours. Then isolated cardiomyocytes and mitochondria were simultaneously treated with (1) control (0.05 % ethanol), (2) celecoxib (20 µg/ml) treatment, (3) celecoxib (20 µg/ml) + CuCsSLN (1 µg/ml) treatment, (4) CuCsSLN (1 µg/ml) treatment, (5) celecoxib (20 µg/ml) + curcumin (10 µM) treatment and (6) curcumin (10 µM) treatment for 4 h at 37 °C. The results showed that celecoxib (20 µg/ml) induced a significant increase in cytotoxicity, reactive oxygen species (ROS) formation, mitochondria membrane potential (ΔΨm) collapse, lipid peroxidation, oxidative stress and mitochondrial swelling while CuCsSLN and curcumin reverted the above toxic effect of celecoxib. Our data indicated that the effect of CuCsSLN in a number of experiments, is significantly better than that of curcumin which shows the role of chitosan nanoparticles in increasing effect of curcumin.

Introduction

The systems of nano delivery and nanomedicine are a new and developing science. These materials are used to deliver therapeutic agents to specific targeted sites in a controlled manner and as diagnostic tools in the nanoscale range [1]. Nanotechnology-based drug delivery systems suggests multiple benefits in preventing and treating human diseases by target-oriented delivery and site-specific of precise medicines [2]. Recently, there are a number of prominent uses of the nanoparticles and nanomedicine in the treatment of different diseases such as biological agents, chemotherapeutic agents, immunotherapeutic agents etc. [3]. The chitosan-coated solid lipid nanoparticles are biocompatible and biodegradable nanocarriers which composed from a lipid core that coated with chitosan polymer chains. This connection is stabilized via electrostatic interactions between anionic surface of lipids and protonated

amine functional groups of chitosan. These nanoparticles showed the advantageous of both constituents: SLNs and chitosan. SLNs have the capability of loading lipophilic active ingredients which composed the majority of current drugs, Chitosan nanoparticles are used and approved for wound dressing applications, sustained release and mucoadhesive chitosan dosage forms [4]. The chitosan-based nanoparticles have been used as a carrier for drug delivery through various routes of administration. This chemical has functional groups that can be altered to arrive specific target, this property making it a polymer with an enormous range of potential applications [5]. The chitosan-coated SLNs and chitosan derivatives typically have an adhesive properties and positive surface charge that can adhere to membranes and release the drug payload in in a controlled manner [6]. Also, because of low toxicity of this carrier in both in vitro and some in vivo models, it showed miscellaneous applications in non-parenteral drug delivery for the treatment of cardiovascular diseases (CVDs), gastrointestinal diseases, pulmonary diseases, cancer, drug delivery to the ocular and brain infections [4, 7].

From many years ago, humans have widely used plant-based natural products as medicines for prevention and treatment of various diseases. Approximately, 25 % of the pharmaceutical agents and their derivatives existing now are obtained from natural sources [8]. Despite prominent role of natural products in prevention and treatment of several major diseases, including cardiovascular, diabetes, cancer, microbial, and inflammatory diseases, and other unique advantages, such as good therapeutic potential, low-price, lower toxicity and side effects, because of concerns associated with poor bioavailability, poor absorption in the body poor, solubility, in vivo instability and issues with target-specific delivery, pharmaceutical companies are hesitant to invest more in natural product-based drug [9]. In consequence, many natural products are not clearing the clinical trial phases because of these problems [10, 11]. Hence, using novel nanotechnology-based drug delivery systems for targeting the specific targets in cell and body could be an option that might solve above mentioned problems [12]. Nanotechnology employs curative agents with sizes ranged between 1 and 100 nm (nanoscale level) to develop nanomedicines [13, 14]. Nanomedicines indicate higher bioavailability because they show typical uptake mechanisms of absorptive endocytosis [15]. Therefore, nanotechnology has a significant role in advanced medicine formulations, targeting, controlled drug release and delivery with massive success.

Celecoxib (CEL) as a selective cyclooxygenase-2 (COX-2) inhibitors has the potential of the cardiotoxic effects [16]. Celecoxib may cause a significant increase in critical cardiotoxic effects, such as congestive heart failure, stroke or myocardial infarction [17, 18]. It has been reported that serious cardiovascular events in patients receiving celecoxib is approximately 2.5 % [19]. The unpleasant cardiovascular effects of nonsteroidal anti-inflammatory drug (NSAIDs) may be due to the oxidative stress [20]. Published data have been demonstrated that NSAIDs induce ROS and mitochondrial damages in different cell types including cardiac related cells and cardiomyocytes [20]. Also, it is concluded that NSAIDs promote the mitochondrial permeability transition under conditions of oxidative stress [21]. It is evident that mitochondrial dysfunction is at the core of cardiovascular toxicity induced by some NSAIDS [22]. Recently, the oxidative stress and mitochondria-related mechanisms of drug-induced cardiotoxicity have been extensively studied [17]. Accumulated data indicates that natural products such as curcumin have great effects in preventing and treating oxidative stress and mitochondria-mediated cardiotoxicity [23]. Curcumin has the cardioprotective effect against cardiotoxicity induced by drugs and chemicals [24]. It has been reported that curcumin scavenges superoxide anion and hydroxyl radicals and inhibits lipid peroxidation [25]. Therefore, in the current study, for the first time, we prepare curcumin-loaded chitosan nanoparticles and evaluate their potential protective against celecoxib-induced cytotoxicity and mitochondrial toxicity on isolated rat heart mitochondria and cardiomyocytes.

Materials and Methods

Preparation of Chitosan Nanoparticles

Solid lipid nanoparticles were prepared using solvent dispersion technique. First an organic phase consisting stearic acid (SA, 150 mg), glyceryl mono stearate (GMS, 50 mg) and curcumin (20 mg) in 20 ml of Ethanol was prepared and after solution of all ingredients with the aid of temperature, this phase was diffused dropwise into 100 ml of an aqueous phase containing 2 % of tween 80 as the surfactant under stirring at 1000 rpm. The temperature of two phases were kept constant at 60 °C until the addition of ethanolic phase was done. After that, the heating was stopped until the mixture reached to room temperature. The formed SLNs were collected for further applications.

To coat the surface of SLNs with chitosan polymer, 25 ml of SLNs mixture was added dropwise to 25 ml of 0.2 % chitosan in acetic acid 0.6 % solution under stirring at 500 rpm. After completion of addition, the stirring was continued for 10 min more to form the chitosan-coat SLNs. The nanoparticles were centrifuged at 9000 rpm for 10 min. The supernatant was discarded and the precipitate was lyophilized and kept for further characterizations.

Characterization of chitosan nanoparticles

To determine the entrapment efficiency (EE) of curcumin in nanoparticles, the concentration of curcumin in supernatant phase of SLNs was measured using spectrophotometric analysis at 2.. nm. The entrapment efficiency was calculated using the following equation:

The drug loading efficiency (DLE) determines the ratio of loaded-drug weight to nanoparticle weight. This parameter was measured in SLNs through dissolution of predetermined amount of lyophilized powder of curcumin-loaded SLNs in specified volume of ethanol and subsequent analysis of curcumin concentration as mentioned above. The equation for calculation of DLE is as follow:

Particle size and particle size distribution analysis of SLNs and CuCs SLNs were done with diffraction light scattering (DLS) technique using Horiba SZ100 instrument (Japan). This method was also utilized to assess the surface charge factor of nanoparticles or zeta potential. The morphology of SLNs and CuCsSLNs was studied using scanning electron microscopy (SEM) analysis (TESCAN model Mira III). The freeze-dried nanoparticles were coated with gold and their surface properties were examined.

The release pattern of curcumin from CuCsSLN was studied using dialysis bag method. Precise weighted number of nanoparticles was poured into prepared dialysis bags. These bags were immersed and suspended in phosphate buffer saline (PBS) as release media. The release test has been done in constant temperature at 37 °C and stirring condition (50 rpm). At predetermined intervals, 1 mL of this media was picked and the curcumin concentration was measured spectrophotometrically at 421 nm. The release diagram was plotted as cumulative percent of loaded curcumin against time.

Animals

Nine-week-old adult male Wistar rats (200–250 g each) were purchased from the Pasteur Institute of Iran (Tehran, Iran). Animals were maintained on standard lab diet and housed in polycarbonate cages in a room free from any source of chemical contamination, thermally controlled (25 ± 1 °C) and artificially illuminated (12 h dark/light cycle) at the Animal House of School of Pharmacy, Ardabil University of Medical Sciences, (Ardabil, Iran). All animals were received humane care in compliance with the guidelines of the Ethics Committee of Ardabil University of Medical Sciences (ethics code: IR.ARUMS.REC.1398.355)

Chemicals and Reagents

Bovine Serum Albumin (BSA), Monopotassium phosphate, 2-Amino-2-hydroxymethyl-propane-1,3-diol (TRIS), Collagenase (Type II), Fetal Bovine Serum (FBS), 199 Medium, N-(2-hydroxyethyl) piperazine-N′-(2-ethanesulfonic acid) (HEPES), Penicillin and Streptomycin Solution,4,5-dimethylthiazol-2-yl)-2,5-diphenyltetrazolium bromide (MTT), Acridine Orange, 3-morpholinopropane-1-sulfonic acid (MOPS),Rhodamine123, Trypan blue, Hank's Balanced Salt Solution (HBSS), Sucrose, 2′,7′-Dichlorofuorescin Diacetate (DCFH-DA), Carnitine, Creatine, Taurine, Butylated hydroxytoluene (BHT), Dimethyl sulfoxide (DMSO), D-mannitol, Potassium chloride, Sodium succinate, Rotenone, Magnesium chloride, and Curcumin with purity 99 % were purchased from Sigma (St. Louis, MO USA). Celecoxib with CAS number 169590–42–5 and a purity of about 99 %, was gifted from Zahravi Pharmaceutical Company, Iran. It was freshly prepared before use and dissolved in normal saline 0.9 % w/v.

Adult Rat Cardiomyocyte Isolation

Adult ventricular cardiomyocytes were isolated from adult male Wistar rats. Rats were intraperitoneally anesthetized with combination of ketamine (50 mg/kg) and xylazine (10 mg/kg). After rats appeared calm, hearts were quickly excised, and directly perfused on a modified Langendorff perfusion apparatus with Powell medium (containing: 110 mM NaCl, 1.2 $MgSO_4$ $7H_2O$, 2.5 mM KCl, 1.2 mM KH_2PO_4, 25 mM Hepes and 10 mM D (+)-Glucose monohydrate in ultra-pure sterile water with pH = 74 adjusted with 2 M NaOH) for 5 mins. Powell medium were replaced by enzyme mixtures containing 30 µM $CaCl_2$ and 5 mg/ml collagenase, in warm Powell medium for 25 minutes. Then, hearts were dissected mechanically to small pieces and shaken in flasks with enzyme mixture for another 10 minutes. The collagenase digested ventricle suspensions were then filtered through a sieve (180 µm) to remove remnants of connective tissues. After rinsing with Powell medium, cell suspensions were placed on top of BSA solution where non-cardiomyocytes were removed by a density gradient. Isolated cardiomyocytes were suspended in CCT medium containing taurine, creatine and carnitine in medium 199 supplemented with antibiotics (100 µg/ml penicillin and 100 µg/ml streptomycin) at 37 °C under a 5 % CO_2 – 95 % air atmosphere. One hour after plating, the CCT medium was changed to remove unattached dead [26].

Cell treatments

Isolated cardiomyocytes were incubated with celecoxib and/or CuCsSLN (1 ml of CuCsSLN suspension containing 1 µg of curcumin), curcumin (3.6 µg/ml) in 5 % CO_2 at 37 °C for 4 h. In our study we have six treatment groups including: (1) control (0.05 % ethanol), (2) celecoxib (20 µg/ml) treatment, (3) celecoxib (20 µg/ml) + CuCsSLN (1 µg/ml) treatment, (4) CuCsSLN (1 µg/ml) treatment, (5) celecoxib (20 µg/ml) + curcumin (3.6 µg/ml) treatment and (6) curcumin (3.6 µg/ml) treatment, all group incubated in CCT medium supplemented with 10 % FBS and antibiotics (100 µg/ml streptomycin and 100 µg/ml penicillin) at 37 °C under a 5 % CO_2 – 95 % air atmosphere. After 4 h of treatment, the cells were collected for cell viability, ROS formation, mitochondrial and lysosomal damages, GSH depletion and lipid peroxidation analysis.

Detection of Cell Viability in Isolated Cardiomyocytes

Isolated cardiomyocytes viability was determined by MTT assay. Isolated cardiomyocytes were treated with MTT at 0.5 mg/ml. The purple formazan crystals were dissolved in DMSO. Solutions were then loaded in a 96 well plate, and determined on an automated microplate spectrophotometer at 570 nm. Each condition tested was performed in triplicate in each experiment. All experiments were performed in three separate experiments [27].

Detection of Reactive Oxygen Species (ROS) in Isolated Cardiomyocytes

ROS generation in isolated cardiomyocytes was detected by DCFH-DA [28, 29]. After 4 hours of incubation, isolated cardiomyocytes were washed with PBS and suspended in PBS containing 5 µM DCF-DA. Aliquots of the isolated cardiomyocytes suspension that were previously stained with DCF-DA were isolated from the incubation medium by 1 min centrifugation at 1000 rpm. Cardiomyocytes washing was performed twice to delete the fluorescent dye from the CCT medium. Afterwards, ROS generation was measured by flow cytometry (Cyflow Space-Partec) and mean of fluorescence intensities of DCF were compared between treated groups.

Detection of Mitochondrial Membrane Potential Collapse in Isolated Cardiomyocytes

The fluorescent dye rhodamine 123, which selectively accumulates in mitochondria was used for detection of ΔΨm collapse in isolated cardiomyocytes. After 4 hours of incubation, the isolated cardiomyocytes were washed with PBS and suspended in PBS containing 5 µM rhodamine 123. The isolated cardiomyocytes suspension that was previously stained with rhodamine 123 were isolated from the CCT medium by centrifugation at 1000 rpm for 1 min. The isolated cardiomyocytes were washed by PBS twice to delete the fluorescent dye from the media. Afterwards, ΔΨm collapse was measured using flow cytometry (Cyflow Space-Partec) and the mean of fluo-

rescence intensities of rhodamine 123 were compared between treated groups [30].

Detection of Lysosomal Membrane Stability in Isolated Cardiomyocytes

The redistribution of the fluorescent dye, acridine orange (AO) was used for detection of lysosomal membrane stability in isolated cardiomyocytes. After 4 hours of incubation, the isolated cardiomyocytes were washed with PBS and suspended in PBS containing 5 µM acridine orange. The isolated cardiomyocytes suspension that was previously stained with acridine orange were isolated from the incubation medium by centrifugation at 1000 rpm for 1 min. The cells were washed by PBS twice to delete the fluorescent dye from the CCT medium. Afterwards, lysosomal membrane stability were detected by flow cytometry (Cyflow Space-Partec) and mean of fluorescence intensities of AO were compared between treated groups [30].

Detection of GSH and GSSG Content in Isolated Cardiomyocytes

Isolated cardiomyocytes reduced glutathione (GSH) and oxidized glutathione (GSSG) content was determined by Hissin and Hilf method [31]. After 4 hours of incubation, the isolated cardiomyocytes were washed with PBS twice and resuspended in 1 mL of phosphate buffer (0.1 mol/L with pH 7.4) and using homogenizer mechanically lysed. The lysed cells were centrifuged at 8,000 × g at 4 °C for 10 min and supernatants were collected. For determination of GSH, 100 µl supernatant was mixed with 3 ml 500 mM TRIS–HCl (pH 8.0) buffer containing 10 mM DTNB and incubated at 25 °C for 15 min. Also, for determination of GSSG, 100 µl of supernatant was added to 3 ml of reaction solution containing 500 mM TRIS–HCl (pH 8.0) buffer, glutathione reductase (1 U for each 3-ml reaction solution), 3 mM $MgCl_2$, 1 mM EDTA, 150 µM NADPH, then was add 100 mM DTNB to a final concentration of 10 mM and incubate at 25 °C for 15 min. The absorbance of developed color was determined at 412 nm by spectrophotometer (BioTek, USA).

Detection of Malondialdehyde Content in Isolated Cardiomyocytes

Isolated cardiomyocytes lipid peroxidation was measured by detecting the amount of malondialdehyde (MDA) formed during the decomposition of fatty acids within cells. After 4 hours of incubation, the isolated cardiomyocytes were washed with PBS, and using homogenizer mechanically lysed in a tube containing 1 ml 0.1 % (w/v) trichloroacetic acid (TCA). Afterwards, the lysate was centrifugate at 10,000 x g for 10 min, the supernatant transferred to new tube containing 4 ml of 20 % TCA containing 0.5 % TBA. The supernatant was boiled in above mixture for 15 minutes at 90 °C. After quick cooling, the mixture was centrifuged at 1000 × g for 10 min. Calorimetric absorption of supernatant was measured at 532 nm [32].

Mitochondrial Isolation

After deep anesthesia, the heart was dissected, chopped, cleared from blood and minced with 10 ml glass homogenizer in the isolation buffer (225 mM D-mannitol, 75 mM sucrose, and 0.2 mM EDTA, pH 7.4) on ice. The obtained samples were centrifuged at 1000 g for 10 minutes and the pellet was removed. The supernatant with mitochondria was poured into ice-cold tube, followed by centrifugation at 10000 g for 10 minutes [33]. The mitochondrial enriched pellets were suspended in appropriate buffer for each test including succinate dehydrogenase activity and mitochondrial swelling.

Mitochondria treatments

Isolated mitochondria were incubated with celecoxib and/or CuCsSLN, curcumin in appropriate buffer at 37 °C for 1 hour. In here we have six treatment groups including: (1) control (0.05 % ethanol), (2) celecoxib (20 µg/ml) treatment, (3) celecoxib (20 µg/ml) + CuCsSLN (1 µg/ml) treatment, (4) CuCsSLN (1 µg/ml) treatment, (5) celecoxib (20 µg/ml) + curcumin (3.6 µg/ml) treatment and (6) curcumin (3.6 µg/ml) treatment. After 1 hour of treatment, the isolated mitochondria were collected for SDH activity and mitochondrial swelling.

Detection of Succinate Dehydrogenase Activity in Isolated Mitochondria

MTT reduction at 570 nm was used for detection of the SDH activity in isolated mitochondria. Briefly, after incubation of rat heart isolated mitochondria in assay buffer (3 mM HEPES, 5 mM succinate, 70 mM sucrose, 2 mM Tris-phosphate, 230 mM mannitol and 1 µM of rotenone) with celecoxib and/or CuCsSLN, curcumin at 37 °C for 60 min. After 1 hour of incubation 0.4 % MTT was added and incubated at 37 °C for 30 min. The purple formazan crystals were dissolved in DMSO and the absorbance was measured at 570 nm [34, 35].

Detection of Mitochondrial Swelling in Isolated Mitochondria

Swelling of mitochondria as an indicator of mitochondrial permeability transition pore (mPTP) opening was determined by monitoring the decrease in light scattering at 540 nm [36, 37]. Rat heart isolated mitochondria were incubated at 37 °C in 100 µl buffer containing 230 mM mannitol, 70 mM sucrose, 3 mM HEPES, 5 mM succinate, 2 mM Tris-phosphate and 1 µM of rotenone. The absorbance was monitored at 540 nm during 60 min.

Statistical Analysis

The statistical analysis was performed by two-way ANOVA, followed by Tukey test, through GraphPad Prism version 5. p- Values of less than 0.05 were considered significant. All experiments were carried-out in triplicate. The flow cytometric data was obtained with Cyflow Space-Partec and analyzed by FlowJo.

Results

Characterization of CNPs

The mean particle size and particle size distribution analysis of nanoparticle samples (one sample from triplicate measuring) have been shown in ▶ **Fig. 1a–d**. As it was seen, curcumin-loaded SLNs had mean particle sizes about 145 ± 11 nm and polydispersity index (PI) of 0.31 ± 0.08. Chitosan-coating caused an increase in particle size up to 208 ± 9 nm and PI = 0.34 ± 0.07. This process also caused an inversion of surface nanoparticle charges from negative values

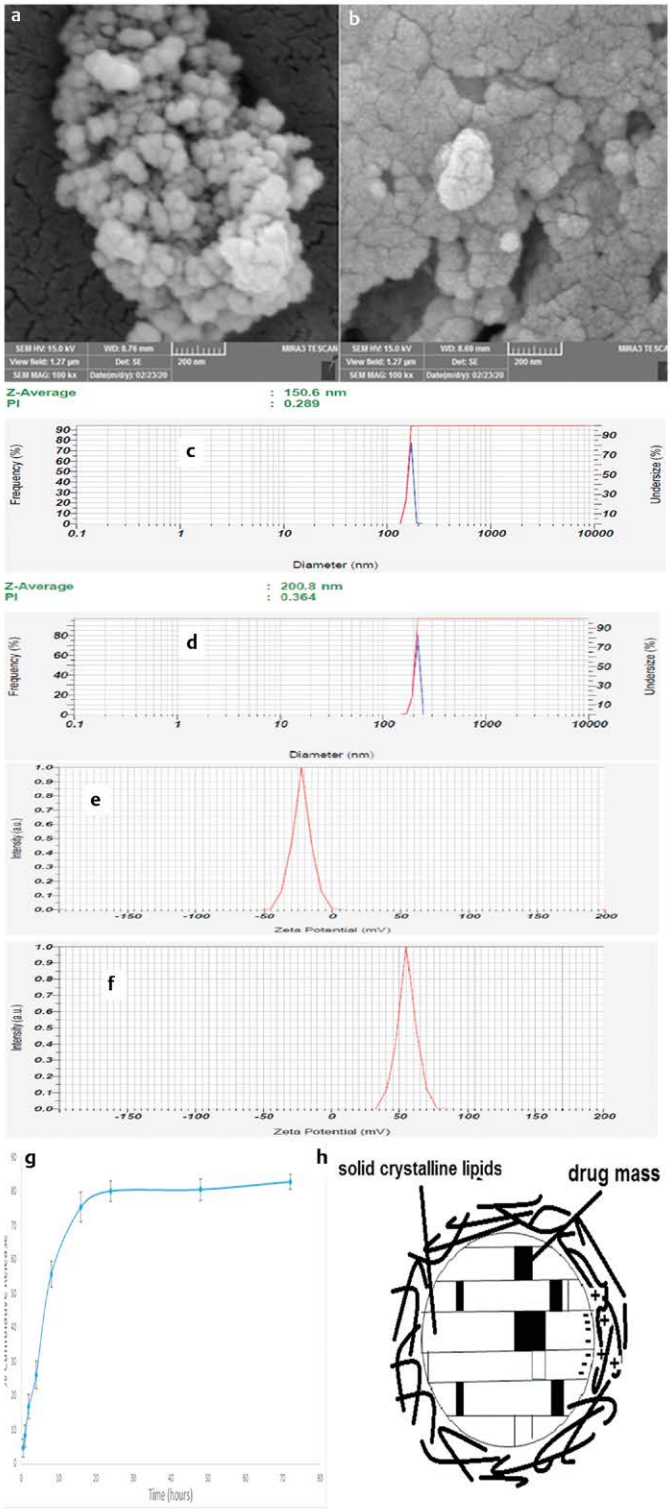

▶ **Fig. 1** SEM image of CuCsSLNs (**a**) and SLNs (**b**). Particle size distribution of SLNs (**c**) and CuCsSLNs (**d**). Zeta potential of SLNs (**e**) and CuCsSLNs (**f**). Release profile of curcumin from CuCsSLNs (**g**). A schematic representation of CsSLNs. The negative surface of SLNs was coated with positively charged chitosan chains (**h**).

in SLNs (−21.5 ± 1.4 mV) to positive values in CsSLNs (+ 53.5 ± 3.7 mV). The nanoscale dimension of nanoparticles was confirmed using SEM image. SEM image of CuCsSLN have been shown in ▶ **Fig. 1e**. This image verifies the nanoscale dimension of nanocarriers. These nanoparticles were homogenous, spherical and with distinct smooth surface.

The results of loading experiments showed that 91.4 ± 3.3 % of used curcumin was incorporated into nanoparticles. The ratio of loaded drug weight to nanocarrier weight which specifies the drug loading efficiency was 12 ± 1.3 %. The release diagram of curcumin from CuCsSLN has been shown in ▶ **Fig. 1f**. As it is seen, the curcumin was released from nanocarrier under a sustain manner. There is not seen any significant burst release of curcumin in release profile. The release of curcumin was continued with a relatively constant slope until 24 hours until that it is reached to a steady state condition at about 80 % cumulative drug release.

Celecoxib-Induced Cytotoxicity Was Ameliorated by CuCsSLN

The results of cell viability on the isolated cardiomyocytes, are indicated in ▶ **Fig. 2a**. There is a significant decrease in cell viability in the celecoxib group as compared with control group ($P < 0.001$). The groups which were cotreated with celecoxib (20 µg/ml) + CuCsSLN (1 µg/ml) and celecoxib (20 µg/ml) + curcumin (10 µM) remained more viable in comparison with celecoxib group ($P < 0.01$). Also, the group which were cotreated with celecoxib (20 µg/ml) + CuCsSLN (1 µg/ml) remained more viable in comparison with celecoxib (20 µg/ml) + curcumin (10 µM) ($P < 0.05$). No significant decrease in the isolated cardiomyocytes viability was observed when the cells were treated with CuCsSLN (1 µg/ml) and curcumin (10 µM) alone as compared with control group.

Celecoxib-Induced Lipid Peroxidation Was Decreased by CuCsSLN

There was a significant elevation in MDA ($P < 0.001$) in celecoxib group in comparison with control (▶ **Fig. 2b**). The groups which were cotreated celecoxib (20 µg/ml) + CuCsSLN (1 µg/ml) and celecoxib (20 µg/ml) + curcumin (10 µM) showed apparent reductions in MDA when compared with celecoxib group ($P < 0.001$), but no difference in MDA levels was observed when compared both group celecoxib (20 µg/ml) + CuCsSLN (1 µg/ml) and celecoxib (20 µg/ml) + curcumin (10 µM) together. Also, no significant changes in the MDA levels were observed when the isolated cardiomyocytes were treated with CuCsSLN (1 µg/ml) and curcumin (10 µM) alone as compared with control group.

Celecoxib-Induced Glutathione Depletion Was Reduced by CuCsSLN

The contents of GSH and GSSG significantly ($p < 0.001$) increased and decreased respectively in the isolated cardiomyocytes treated with celecoxib (20 µg/ml). A significant recovery ($p < 0.001$) in GSH content and a significant decrease in GSSG was observed when the isolated cardiomyocytes cotreated with celecoxib (20 µg/ml) + CuCsSLN (1 µg/ml) and celecoxib (20 µg/ml) + curcumin (10 µM) in comparison with celecoxib group ($P < 0.001$), but did not observe significant different in the contents of GSH and GSSG when compared both group celecoxib (20 µg/ml) + CuCsSLN (1 µg/ml) and celecoxib (20 µg/ml) + curcumin (10 µM) together. CuCsSLN (1 µg/ml) and curcumin (10 µM) alone did not show any change in the isolated cardiomyocytes GSH content and GSSG when compared with control group (▶ **Fig. 2c–d**).

Celecoxib-Induced ROS Formation Was Reduced by CuCsSLN

As shown in ▶ **Fig. 3**, ROS formation considerably increased in celecoxib group when compared to control group ($P < 0.001$). However, cotreatment with celecoxib (20 µg/ml) + CuCsSLN (1 µg/ml) and celecoxib (20 µg/ml) + curcumin (10 µM) significantly decreased ROS formation ($P < 0.001$) in comparison with celecoxib ($P < 0.001$), but did not observe significant different in mean of fluorescence intensity of DCF when compared both group celecoxib (20 µg/ml) + CuCsSLN (1 µg/ml) and celecoxib (20 µg/ml) + curcumin (10 µM) together. No significant changes in the isolated cardiomyocytes ROS formation were observed when the isolated cardiomyocytes were treated with CuCsSLN (1 µg/ml) and curcumin (10 µM) alone as compared with control group.

Celecoxib-Induced Mitochondrial Damages Was Decreased by CuCsSLN

As shown in ▶ **Fig. 4**, following celecoxib treatment (20 µg/ml), the fluorescence intensity of rhodamine-123, as an indicator of MMP collapse, increased significantly in the isolated cardiomyocytes as compared to the control group ($P < 0.001$). However, the fluorescence intensity of rhodamine-123 was significantly decreased ($P < 0.001$) when the isolated cardiomyocytes cotreated with celecoxib (20 µg/ml) + CuCsSLN (1 µg/ml) and celecoxib (20 µg/ml) + curcumin (10 µM) in comparison with celecoxib group ($P < 0.001$), but did not observe significant different in mean of fluorescence intensity of rhodamine-123 when compared both group celecoxib (20 µg/ml) + CuCsSLN (1 µg/ml) and celecoxib (20 µg/ml) + curcumin (10 µM) together. Also, no significant alteration in MMP collapse was observed when the isolated cardiomyocytes were treated with CuCsSLN (1 µg/ml) and curcumin (10 µM) alone as compared with control group.

Celecoxib-Induced Lysosomal Membrane Destabilization Was Ameliorated by CuCsSLN

As shown in ▶ **Fig. 5**, following celecoxib treatment (20 µg/ml), the fluorescence intensity of acridine orange, as an indicator of lysosomal membrane destabilization, increased significantly in the isolated cardiomyocytes as compared to the untreated control group ($P < 0.001$). However, the fluorescence intensity of acridine orange was significantly reduced ($P < 0.001$) when the isolated cardiomyocytes cotreated with celecoxib (20 µg/ml) + CuCsSLN (1 µg/ml) and celecoxib (20 µg/ml) + curcumin (10 µM) in comparison with celecoxib group ($P < 0.001$), but did not observe significant different in the fluorescence intensity acridine orange when compared both group celecoxib (20 µg/ml) + CuCsSLN (1 µg/ml) and celecoxib (20 µg/ml) + curcumin (10 µM) together. Also, no significant change in the fluorescence intensity of acridine orange, as an indicator of lysosomal membrane destabilization was observed when the isolated cardiomyocytes were treated with CuCsSLN (1 µg/ml) and curcumin (10 µM) alone as compared with control group.

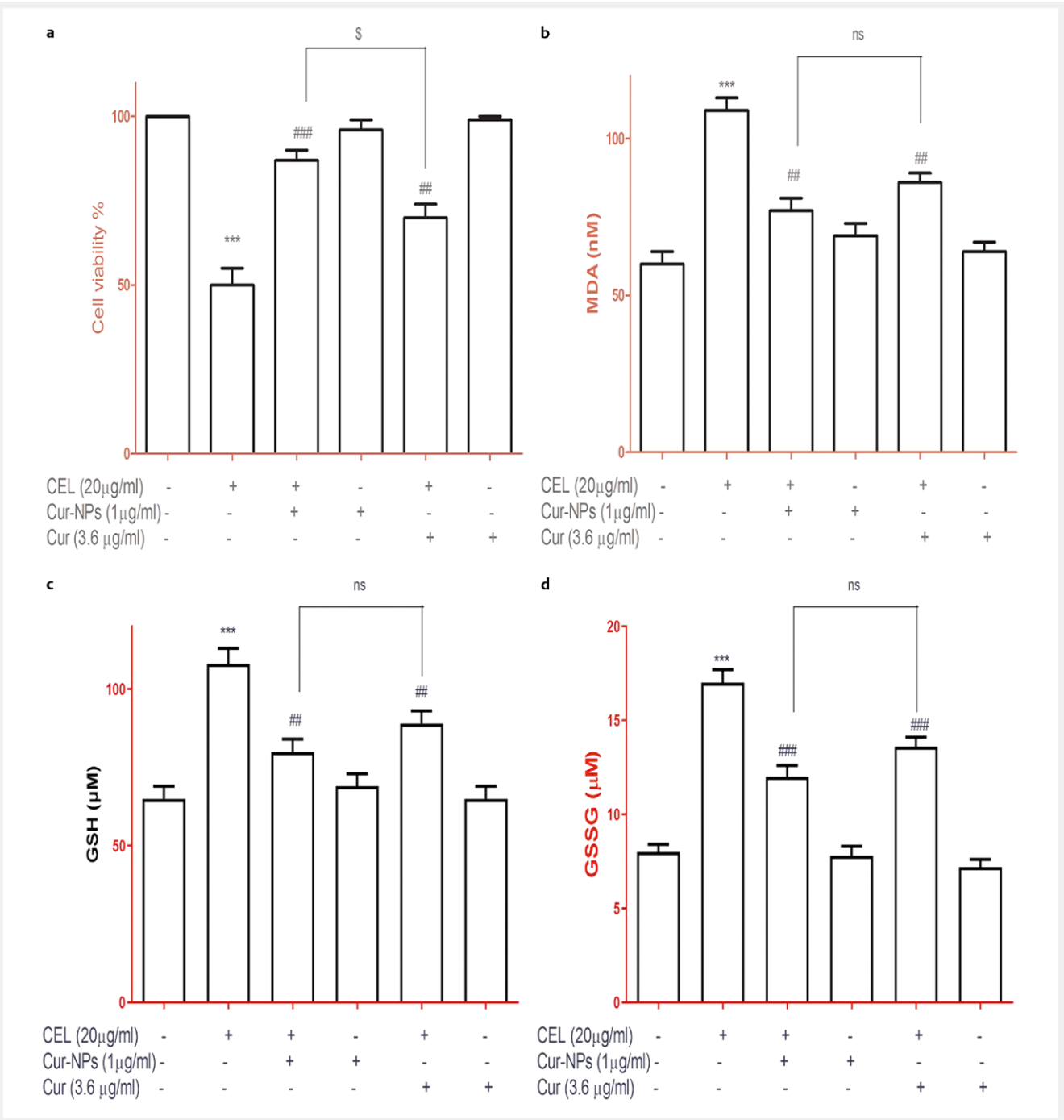

▶ **Fig. 2** CuCsSLN and curcumin reduce cytotoxicity GSH depletion induced by celecoxib in rat isolated cardiomyocytes. (**a**) Representative MTT assay rat isolated cardiomyocytes treated with celecoxib (20 µg/ml), CuCsSLN and curcumin at 4 hours. (**b**) Addition of CuCsSLN and curcumin decreases celecoxib-induced lipid peroxidation in rat isolated cardiomyocytes. Representative measurements of lipid peroxidation following celecoxib exposure (4 h) in the presence or absence of CuCsSLN or curcumin in rat isolated cardiomyocytes. (**c**) GSH content significantly decreased in celecoxib-treated rat isolated cardiomyocytes while cotreatment CuCsSLN or curcumin with celecoxib obviously increased the GSH content in rat isolated cardiomyocytes. (**d**) Also, celecoxib significantly increased the GSSG content in rat isolated cardiomyocytes after 4 h of exposure while CuCsSLN or curcumin significantly decreased the GSSG content in the presence of celecoxib. Results are shown as mean ± SD, n = 3 technical replicates. All experiments were repeated at least three times. *** $p < 0.001$: control versus celecoxib; ###$p < 0.001$: celecoxib + CuCsSLN or curcumin versus celecoxib-treated rat isolated cardiomyocytes; ANOVA, Tukey's test.

Mitochondrial functionality in Isolated Mitochondria

The results of SDH activity on the isolated mitochondria, are shown in ▶ **Fig. 6a**. There is a significant decrease in SDH activity in celecoxib (20 µg/ml) group as compared with control group ($P < 0.001$). The groups which were cotreated with celecoxib (20 µg/ml) + CuCsSLN (1 µg/ml) and celecoxib (20 µg/ml) + curcumin

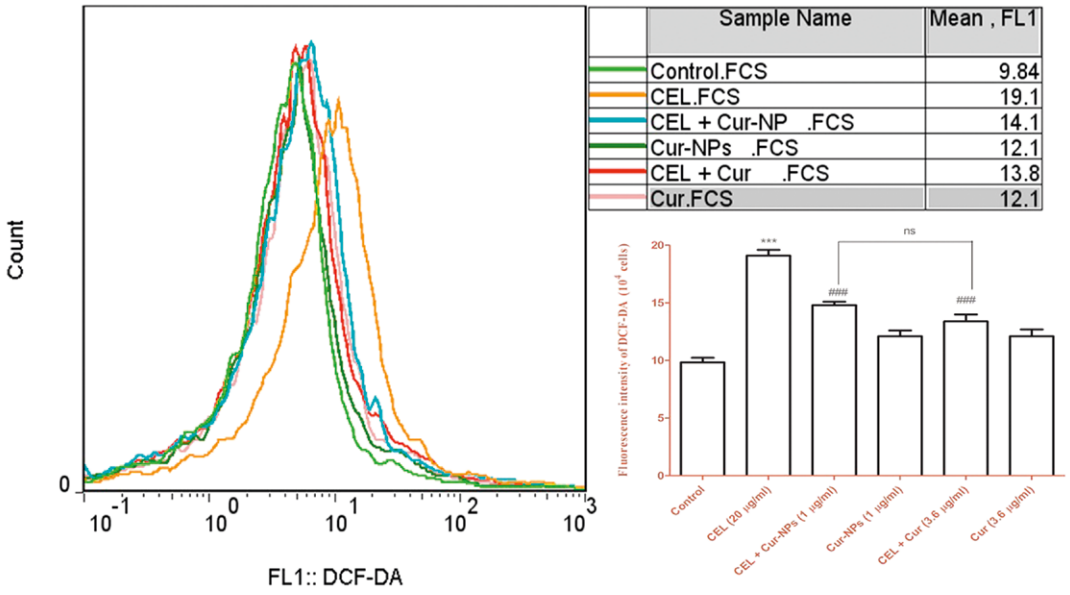

▶ **Fig. 3** CuCsSLN and curcumin decrease mitochondrial ROS formation. Mitochondrial ROS formation was analyzed by means of fluorescence intensity of DCFH-DA following celecoxib exposure (4 hours) in the presence or absence of CuCsSLN or curcumin in rat isolated cardiomyocytes. Bar graphs with statistics. Data are presented as mean ± SD, n = 3, independent experiments repeated at least 3 times, *** p < 0.001: control versus celecoxib; ###p < 0.001: celecoxib + CuCsSLN or curcumin versus celecoxib-treated rat isolated cardiomyocytes; ANOVA, Tukey's test.

(10 µM) increased SDH activity in comparison with celecoxib group (P < 0. 01). Also, the group which were cotreated with celecoxib (20 µg/ml) + CuCsSLN (1 µg/ml) increased more SDH activity in comparison with celecoxib (20 µg/ml) + curcumin (10 µM) (P < 0. 01). No significant decrease in the SDH activity was observed when isolated mitochondria were treated with CuCsSLN (1 µg/ml) and curcumin (10 µM) alone when compared with control group.

Celecoxib-Induced Mitochondrial Swelling Was Decreased by CuCsSLN

As shown in ▶ **Fig. 6b**, following celecoxib treatment (20 µg/ml), the decreased absorbance at 540 nm, as an indicator of mitochondrial swelling, decreased significantly in the isolated mitochondria as compared to the control group (P < 0.001). However, the decreased absorbance at 540 nm was significantly increased (P < 0.001) when the isolated mitochondria cotreated with celecoxib (20 µg/ml) + CuCsSLN (1 µg/ml) and celecoxib (20 µg/ml) + curcumin (10 µM) in comparison with celecoxib group (P < 0.001), but did not observe significant different in the decreased absorbance at 540 nm when compared both group celecoxib (20 µg/ml) + CuCsSLN (1 µg/ml) and celecoxib (20 µg/ml) + curcumin (10 µM) together. Also, no significant change in the decreased absorbance at 540 nm was observed when the isolated mitochondria were treated with CuCsSLN (1 µg/ml) and curcumin (10 µM) alone as compared with control group.

Discussion

Our previous studies and other authors have been reported that curcumin shows a wide range of good therapeutic effects including antioxidant, anti-inflammatory, antiviral, anti-fungal, antibacterial, chemoprotective, tissue protective, immuno-modulating, metabolism regulating, anti-depressant and anticancer properties [38]. Issues which greatly limit the usefulness and effectiveness of curcumin are its rapid metabolism to inactive metabolites and low bioavailability attributed to water insolubility [38]. Curcumin practically insoluble at room temperature in water at acidic and neutral pH and it is very susceptible to auto-degradation. Hence, there are various formulations to enhance dispersibility or solubility with the goal of enhancing bio-efficacy and bioavailability of curcumin [38]. Several delivery systems such as nano-emulsions, solid lipid nanoparticles, liposomes, micelles, microemulsions, microgels, phospholipid complexes, emulsions, nanostructured lipid carriers and biopolymer nanoparticles [38]. These delivery systems enhance efficacy and bioavailability of curcumin through preventing possible degradation in the gastrointestinal tract and optimal permeation in the small intestine [38]. In this study, we prepared a curcumin-loaded chitosan nanoparticle to facilitate uptake from the intestinal tract, protecting against rapid metabolism, and increase interaction with cell surface molecules to enter the cell via clathrin mediated endocytosis.

The carriers of nanoparticulate drug/gene have increased much attention in the recent years because of their tunable and versatile properties [39]. Use of materials with properties such as biodegradable, biocompatible, safe and non-toxic can be further enhanced the efficacy of the therapeutic agents [39]. Polysaccharides-based nanoparticles are an emerging class of biopolymers with above mentioned properties. Chitosan is a natural polysaccharide similar to the cellulose with a net positive charge which is composed of repeating units of D-glucosamine [40, 41]. Because of excellent properties of chitosan such as neuroprotective behaviours, anti-inflammatory, natural antibacterial and good biocompatibility, today this

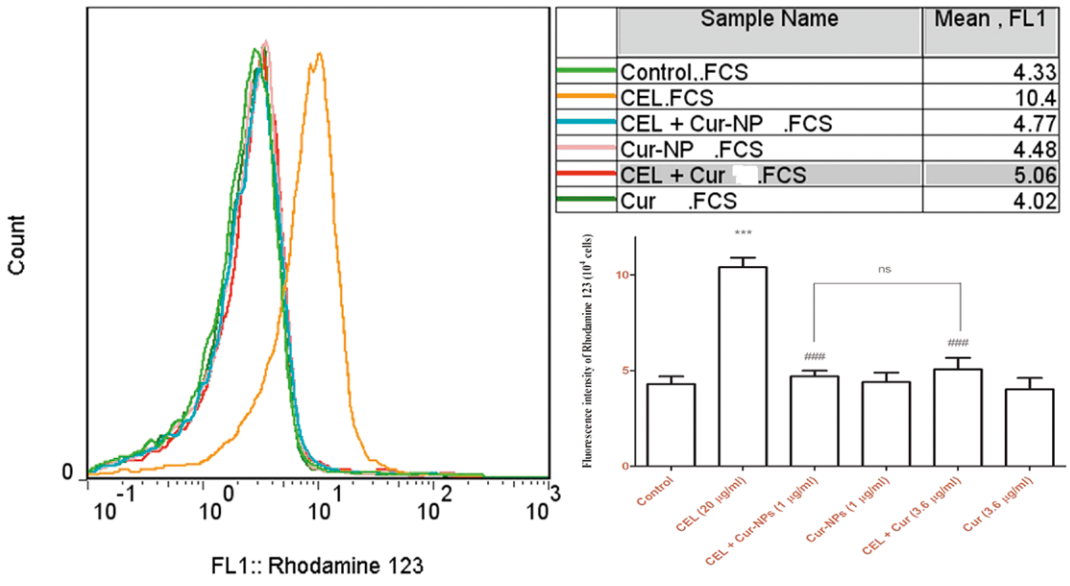

▶ **Fig. 4** CuCsSLN and curcumin decrease mitochondrial damages. Mitochondrial membrane potential collapse was analyzed by means of fluorescence intensity of rhodamine 123 as a cationic dye following celecoxib exposure (4 hours) in the presence or absence of CuCsSLN or curcumin in rat isolated cardiomyocytes. Bar graphs with statistics. Data are presented as mean ± SD, n = 3, independent experiments repeated at least 3 times, *** p < 0.001: control versus celecoxib; ###p < 0.001: celecoxib + CuCsSLN or curcumin versus celecoxib-treated rat isolated cardiomyocytes; ANOVA, Tukey's test.

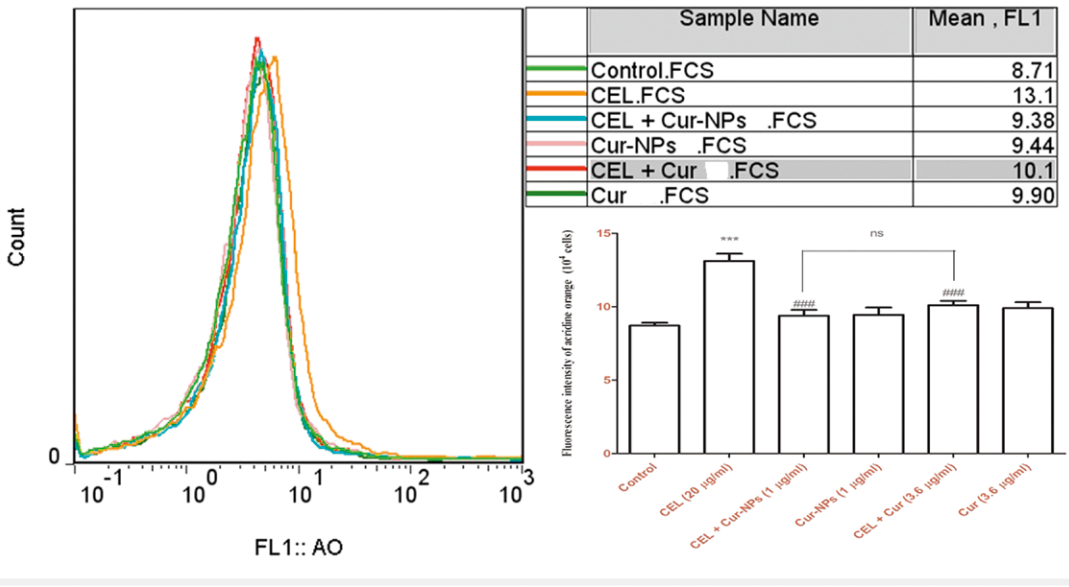

▶ **Fig. 5** CuCsSLN and curcumin decrease lysosomal integrity. Lysosomal integrity was analyzed by means of fluorescence intensity of acridine orange following celecoxib exposure (4 hours) in the presence or absence of CuCsSLN or curcumin in rat isolated cardiomyocytes. Bar graphs with statistics. Data are presented as mean ± SD, n = 3, independent experiments repeated at least 3 times, *** p < 0.001: control versus celecoxib; ###p < 0.001: celecoxib + CuCsSLN or curcumin versus celecoxib-treated rat isolated cardiomyocytes; ANOVA, Tukey's test.

natural polysaccharide is the most common polymer used for drug or gene delivery [42]. In vivo, enzymes such as lysozyme and chitosanase can enzymatically degrade chitosan into to N-glucosamine, which is naturally present in the body [43]. It has been reported that chitosan nanoparticles, because of its net positive charge tend to make interactions with negative charged proteins at the cellular surface and form clathrin vesicles. Then these vesicles slump into the cytoplasm from the plasma membrane and fuse with lysosomes/endosomes compartments. The acidity of the lysosome and presence of enzymes, leads to the breaking of chemical bonds and structure of chitosan nanoparticles and rapid release of burden. Previous studies showed that chitosan nanoparticles

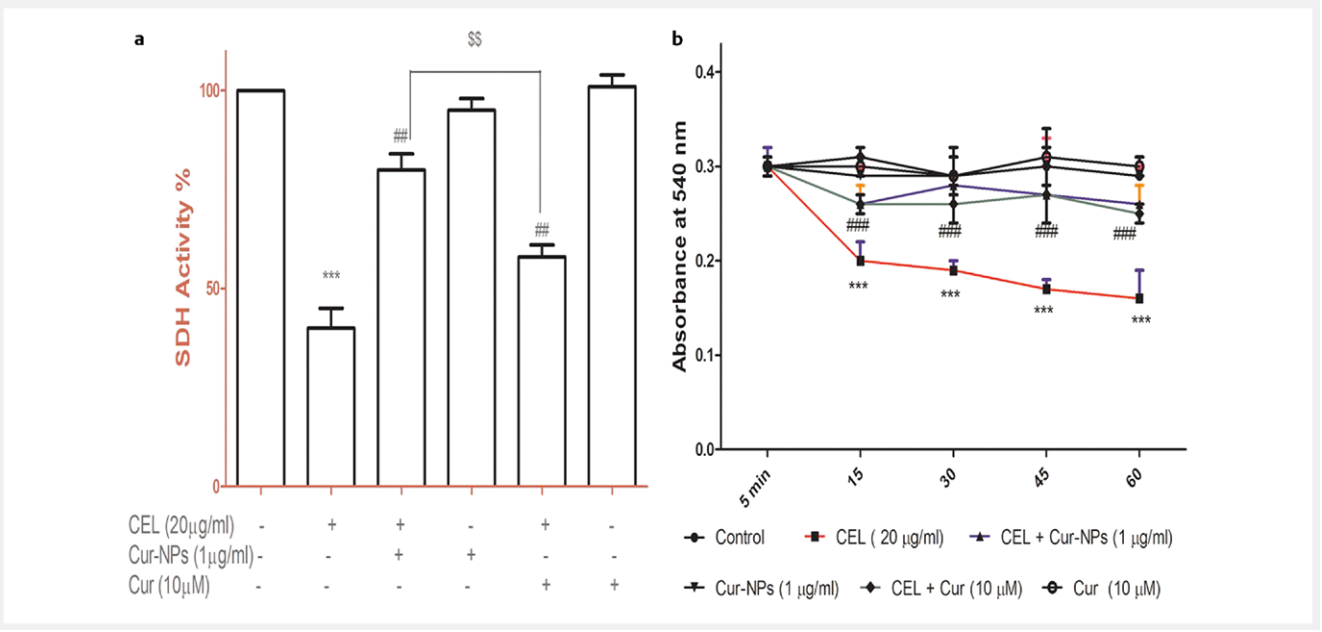

▶ **Fig. 6** CuCsSLN and curcumin increased SDH activity in rat isolated mitochondria after exposure with celecoxib. (**a**) Representative MTT assay rat isolated mitochondria treated with celecoxib (20 μg/ml), CuCsSLN and curcumin at 1 hours. (**b**) Mitochondrial swelling was monitored by following 540 nm absorbance decrease. Celecoxib induced mitochondrial swelling in in isolated rat heart mitochondria in a time depending manner. CuCsSLN and curcumin significantly inhibited mitochondrial swelling compared to treated groups with celecoxib. Results are shown as mean ± SD, n = 3 technical replicates. All experiments were repeated at least three times. *** $p < 0.001$: control versus celecoxib; ###$p < 0.001$: celecoxib + CuCsSLN or curcumin versus celecoxib-treated rat isolated cardiomyocytes; ANOVA, Tukey's test.

with good spherical monodispersity and positive surface increased the cellular uptake of the burden, through the caveolae-mediated endocytosis and macropinocytosis pathway [44]. It has been reported that comparing the cellular uptake of chitosan molecules and chitosan nanoparticles showed two times higher interaction with chitosan nanoparticles than that of chitosan molecules. Previous studies have proved that clathrin is the major route for cellular uptake of the chitosan nanoparticles. It has been reported that clathrin-mediated endocytosis in cardiomyocytes plays a critical role in uptake of exogenous agents [45]. These findings suggest that the nanoscale particles of chitosan results in a greatly improved cellular interaction and transport via cell membrane [46]. In another study has shown that chitosan nanoparticles can cause stronger alterations in the general membrane composition, fluidity of membrane lipids and distribution of membrane proteins [47].

NSAIDs are associated with cardiovascular adverse effects [17]. A loss of heart mitochondrial function is considered as a factor of cardiotoxicity [48]. Mitochondrial membrane permeability transition (mPT) and has been suggested as one of the main mechanisms of drug induced cardiotoxicity [49]. Decline in mitochondrial function has a main role in drug and chemical-induced cardiotoxicity [50]. A recent study showed that celecoxib dose-dependently induced mitochondria swelling, uncoupling activity and increase of the oxygen consumption rate [51]. Also, celecoxib showed exert inhibitory effects on the electron transport chain [51]. Alterations in MMP, decline respiratory chain activity lead to increase mitochondria-based oxidative stress [52]. Our results on rat heart isolated cardiomyocytes and mitochondria showed that celecoxib induces cytotoxicity, ROS formation, mitochondrial and lysosomal damages, depletion of glutathione, oxidative stress, mitochondrial swelling and mitochondrial dysfunction. Our results are consistent with previously published data examining effect of celecoxib on cell and mitochondria.

Use of mitochondrial/lysosomal protective agents and antioxidant seem to be the most promising approaches to protect or treat drug-induced cardiotoxicity [53]. Therefore, more attention has been focused on developing mitochondrial/lysosomal protective agents and antioxidant [53]. Mitochondria are the main site of ROS formation during the enzymatic activity of electron transport chain [54]. Impairment of mitochondrial dynamics and uncontrolled generation of ROS result in mitochondrial damages and structural changes of cellular proteins, lipids, DNA and enzymes [55]. Therefore, a crucial step in the treatment of a cardiotoxicity is targeting of oxidative stress and mitochondrial dysfunction by antioxidants and mitochondrial protective agents. To protect oxidative stress and mitochondrial dysfunction, different agents have been introduced and applied to preclinical and clinical studies [56]. In this study we observed that CuCsSLN and curcumin can reduce cellular and mitochondrial toxicity parameters after exposure with celecoxib. It has been reported that curcumin has mitochondrial and cardioprotective effect against doxorubicin-induced injury [57]. Also, curcumin's cardioprotective effects are related with maintaining mitochondrial function [58]. Our results in here is consistent with previously published data examining mitochondrial and cardioprotective of curcumin. In a number of experiments, our data indicated that the effect of CuCsSLN were significantly better than that of curcumin which shows the role of formulation in increasing efficiency of curcumin.

In conclusion, we demonstrated that celecoxib directly induces cytotoxicity, oxidative stress and mitochondrial/lysosomal impairment in isolated cardiomyocytes and mitochondria. Also, we confirmed that CuCsSLN and curcumin has a potential to inhibit cytotoxicity, mitochondrial/lysosomal dysfunction and oxidative stress induced by celecoxib. In a number of experiments, the effect of CuCsSLN were significantly better than that of curcumin which shows the role of chitosan nanoparticles in increasing efficiency of curcumin. The limitation of current study this is which these data must be verified by animal trials and clinical trials, to establish the effects of CuCsSLN and curcumin.

Acknowledgement

The results presented in the current article was extracted from the Pharm D. thesis of Samira Esmaeli. The thesis was conducted under supervision of Dr. Hossein Ali Ebrahimi and Dr. Ahmad Salimi at School of Pharmacy, Ardabil University of Medical Sciences.

Funding Information

This work was supported by Ardabil of Medical Sciences, Deputy of Research with ethics code IR.ARUMS.REC.1398.355.

Conflict of Interest

The authors declare that they have no conflict of interest.

References

[1] Patra JK, Das G, Fraceto LF et al. Nano based drug delivery systems: recent developments and future prospects. Journal of nanobiotechnology 2018; 16: 71

[2] Parveen S, Misra R, Sahoo SK. Nanoparticles: a boon to drug delivery, therapeutics, diagnostics and imaging. Nanomedicine: Nanotechnology, Biology and Medicine 2012; 8: 147–166

[3] Muthu MS, Leong DT, Mei L et al. Nanotheranostics-application and further development of nanomedicine strategies for advanced theranostics. Theranostics 2014; 4: 660

[4] Mohammed MA, Syeda J, Wasan KM et al. An overview of chitosan nanoparticles and its application in non-parenteral drug delivery. Pharmaceutics 2017; 9: 53

[5] Park JH, Saravanakumar G, Kim K et al. Targeted delivery of low molecular drugs using chitosan and its derivatives. Advanced drug delivery reviews 2010; 62: 28–41

[6] Upadhyaya L, Singh J, Agarwal V et al. The implications of recent advances in carboxymethyl chitosan based targeted drug delivery and tissue engineering applications. Journal of Controlled Release 2014; 186: 54–87

[7] Deng Y, Zhang X, Shen H et al. Application of the Nano-Drug Delivery System in Treatment of Cardiovascular Diseases. Frontiers in Bioengineering and Biotechnology 2019; 7

[8] Swamy MK, Sinniah UR. Patchouli (Pogostemon cablin Benth.): botany, agrotechnology and biotechnological aspects. Industrial Crops and Products 2016; 87: 161–176

[9] Beutler JA. Natural products as a foundation for drug discovery. Current protocols in pharmacology 2019; 86: e67

[10] Bonifácio BV, da Silva PB, dos Santos Ramos MA et al. Nanotechnology-based drug delivery systems and herbal medicines: a review. International journal of nanomedicine 2014; 9: 1

[11] Watkins R, Wu L, Zhang C et al. Natural product-based nanomedicine: recent advances and issues. International journal of nanomedicine 2015; 10: 6055

[12] Jahangirian H, Lemraski EG, Webster TJ et al. A review of drug delivery systems based on nanotechnology and green chemistry: green nanomedicine. International journal of nanomedicine 2017; 12: 2957

[13] Patra JK, Baek K-H. Green nanobiotechnology: factors affecting synthesis and characterization techniques. Journal of Nanomaterials 2014; 2014

[14] Arayne MS, Sultana N, Qureshi F. nanoparticles in delivery of cardiovascular drugs. Pakistan journal of pharmaceutical sciences 2007; 20: 340–348

[15] Kou L, Sun J, Zhai Y et al. The endocytosis and intracellular fate of nanomedicines: Implication for rational design. Asian Journal of Pharmaceutical Sciences 2013; 8: 1–10

[16] Mosler C. Cardiovascular risk associated with NSAIDs and COX-2 inhibitors. US Pharm 2014; 39: 35–38

[17] Varga Z. rafay ali Sabzwari S, Vargova V. Cardiovascular risk of nonsteroidal anti-inflammatory drugs: an under-recognized public health issue. Cureus 2017; e1144. doi: 10.7759/cureus.1144

[18] Caldwell B, Aldington S, Weatherall M et al. Risk of cardiovascular events and celecoxib: a systematic review and meta-analysis. Journal of the Royal Society of Medicine 2006; 99: 132–140

[19] Arber N, Eagle CJ, Spicak J et al. Celecoxib for the prevention of colorectal adenomatous polyps. New England Journal of Medicine 2006; 355: 885–895

[20] Ghosh R, Alajbegovic A, Gomes AV. NSAIDs and cardiovascular diseases: role of reactive oxygen species. Oxidative medicine and cellular longevity 2015; 536962. doi: 10.1155/2015/536962

[21] Lal N, Kumar J, Erdahl WE et al. Differential effects of non-steroidal anti-inflammatory drugs on mitochondrial dysfunction during oxidative stress. Archives of biochemistry and biophysics 2009; 490: 1–8

[22] Salimi A, Neshat MR, Naserzadeh P et al. Mitochondrial permeability transition pore sealing agents and antioxidants protect oxidative stress and mitochondrial dysfunction induced by naproxen, diclofenac and celecoxib. Drug research 2019; 69: 598–605

[23] Shabalala S, Muller C, Louw J et al. Polyphenols, autophagy and doxorubicin-induced cardiotoxicity. Life sciences 2017; 180: 160–170

[24] Nabofa WE, Alashe OO, Oyeyemi OT et al. Cardioprotective effects of curcumin-nisin based poly lactic acid nanoparticle on myocardial infarction in guinea pigs. Scientific reports 2018; 8: 1–11

[25] Morin D, Barthélémy S, Zini R et al. Curcumin induces the mitochondrial permeability transition pore mediated by membrane protein thiol oxidation. FEBS letters 2001; 495: 131–136

[26] Xu Q, Ming Z, Dart AM et al. Optimizing dosage of ketamine and xylazine in murine echocardiography. Clinical and Experimental Pharmacology and Physiology 2007; 34: 499–507

[27] Naserzadeh P, Mehr SN, Sadabadi Z et al. Curcumin protects mitochondria and cardiomyocytes from oxidative damage and apoptosis induced by hemiscorpius lepturus venom. Drug research 2018; 68: 113–120

[28] Huang P, Zhang YH, Zheng XW et al. Phenylarsine oxide (PAO) induces apoptosis in HepG2 cells via ROS-mediated mitochondria and ER-stress dependent signaling pathways. Metallomics 2017; 9: 1756–1764

[29] Aghvami M, Ebrahimi F, Zarei MH et al. Matrine Induction of ROS Mediated Apoptosis in Human ALL B-lymphocytes Via Mitochondrial Targeting. Asian Pacific journal of cancer prevention : APJCP 2018; 19: 555–560. doi:10.22034/apjcp.2018.19.2.555

[30] Salimi A, Roudkenar MH, Sadeghi L et al. Selective anticancer activity of acacetin against chronic lymphocytic leukemia using both in vivo and in vitro methods: key role of oxidative stress and cancerous mitochondria. Nutrition and cancer 2016; 68: 1404–1416

[31] Hissin PJ, Hilf R. A fluorometric method for determination of oxidized and reduced glutathione in tissues. Analytical biochemistry 1976; 74: 214–226

[32] Beach DC, Giroux E. Inhibition of lipid peroxidation promoted by iron (III) and ascorbate. Archives of biochemistry and biophysics 1992; 297: 258–264

[33] Huang L, Zhang K, Guo Y et al. Honokiol protects against doxorubicin cardiotoxicity via improving mitochondrial function in mouse hearts. Scientific reports 2017; 7: 1–12

[34] Salimi A, Roudkenar MH, Seydi E et al. Chrysin as an anti-cancer agent exerts selective toxicity by directly inhibiting mitochondrial complex II and V in CLL B-lymphocytes. Cancer investigation 2017; 35: 174–186

[35] Hosseini M-J, Naserzadeh P, Salimi A et al. Toxicity of cigarette smoke on isolated lung, heart, and brain mitochondria: induction of oxidative stress and cytochrome c release. Toxicological & Environmental Chemistry 2013; 95: 1624–1637

[36] Escobales N, Nuñez RE, Jang S et al. Mitochondria-targeted ROS scavenger improves post-ischemic recovery of cardiac function and attenuates mitochondrial abnormalities in aged rats. Journal of molecular and cellular cardiology 2014; 77: 136–146

[37] Salimi A, Nikoosiar Jahromi M, Pourahmad J. Maternal exposure causes mitochondrial dysfunction in brain, liver, and heart of mouse fetus: An explanation for perfluorooctanoic acid induced abortion and developmental toxicity. Environmental toxicology 2019; 34: 878–885. doi:10.1002/tox.22760

[38] Xu X-Y, Meng X, Li S et al. Bioactivity, health benefits, and related molecular mechanisms of curcumin: Current progress, challenges, and perspectives. Nutrients 2018; 10: 1553

[39] Salatin S, Yari Khosroushahi A. Overviews on the cellular uptake mechanism of polysaccharide colloidal nanoparticles. Journal of Cellular and Molecular Medicine 2017; 21: 1668–1686. doi:10.1111/jcmm.13110

[40] Dutta PK, Dutta J, Tripathi V. Chitin and chitosan: Chemistry, properties and applications 2004

[41] Zhou Y, Li J, Lu F et al. A study on the hemocompatibility of dendronized chitosan derivatives in red blood cells. Drug design, development and therapy 2015; 9: 2635

[42] Wu J, Liu G, Qin Y-X et al. Effect of low-intensity pulsed ultrasound on biocompatibility and cellular uptake of chitosan-tripolyphosphate nanoparticles. Biointerphases 2014; 9: 031016

[43] Huang M, Khor E, Lim L-Y. Uptake and cytotoxicity of chitosan molecules and nanoparticles: effects of molecular weight and degree of deacetylation. Pharmaceutical research 2004; 21: 344–353

[44] Zhao L, Yang G, Shi Y et al. Co-delivery of Gefitinib and chloroquine by chitosan nanoparticles for overcoming the drug acquired resistance. Journal of Nanobiotechnology 2015; 13: 57

[45] Eguchi S, Takefuji M, Sakaguchi T et al. Cardiomyocytes capture stem cell-derived, anti-apoptotic microRNA-214 via clathrin-mediated endocytosis in acute myocardial infarction. Journal of Biological Chemistry 2019; 294: 11665–11674

[46] Ma Z, Lim L-Y. Uptake of chitosan and associated insulin in Caco-2 cell monolayers: a comparison between chitosan molecules and chitosan nanoparticles. Pharmaceutical research 2003; 20: 1812–1819

[47] Zheng A-p, Liu H-x, Yuan L et al. Comprehensive studies on the interactions between chitosan nanoparticles and some live cells. Journal of Nanoparticle Research 2011; 13: 4765–4776

[48] [Anonymous]. !!! INVALID CITATION !!! {}

[49] Montaigne D, Hurt C, Neviere R. Mitochondria death/survival signaling pathways in cardiotoxicity induced by anthracyclines and anticancer-targeted therapies. Biochemistry research international 2012; 2012:

[50] Varga ZV, Ferdinandy P, Liaudet L et al. Drug-induced mitochondrial dysfunction and cardiotoxicity. American Journal of Physiology-Heart and Circulatory Physiology 2015; 309: H1453–H1467

[51] Tatematsu Y, Fujita H, Hayashi H et al. Effects of the nonsteroidal anti-inflammatory drug celecoxib on mitochondrial function. Biological and Pharmaceutical Bulletin 2018; 41: 319–325

[52] Davis RE, Williams M. Mitochondrial function and dysfunction: an update. Journal of Pharmacology and Experimental Therapeutics 2012; 342: 598–607

[53] Camara AK, Bienengraeber M, Stowe DF. Mitochondrial approaches to protect against cardiac ischemia and reperfusion injury. Frontiers in physiology 2011; 2: 13

[54] Galluzzi L, Kepp O, Trojel-Hansen C et al. Mitochondrial control of cellular life, stress, and death. Circulation research 2012; 111: 1198–1207

[55] Siasos G, Tsigkou V, Kosmopoulos M et al. Mitochondria and cardiovascular diseases—from pathophysiology to treatment. Annals of translational medicine 2018; 6: 256. doi: 10.21037/atm.2018.06.21

[56] Sheu S-S, Nauduri D, Anders M. Targeting antioxidants to mitochondria: a new therapeutic direction. Biochimica et Biophysica Acta (BBA)-Molecular Basis of Disease 2006; 1762: 256–265

[57] He H, Luo Y, Qiao Y et al. Curcumin attenuates doxorubicin-induced cardiotoxicity via suppressing oxidative stress and preventing mitochondrial dysfunction mediated by 14-3-3γ. Food & Function 2018; 9: 4404–4418

[58] Correa F, Buelna-Chontal M, Hernández-Reséndiz S et al. Curcumin maintains cardiac and mitochondrial function in chronic kidney disease. Free Radical Biology and Medicine 2013; 61: 119–129